7th International Conference on Arch Bridges
ARCH'13
2 - 4 October 2013 Trogir - Split, Croatia
MAINTENANCE, ASSESSMENT AND REPAIR

MODELLING OF MASONRY ARCHES STRENGHTENED WITH COMPOSITE MATERIALS

Stefano De Santis* & Gianmarco De Felice[+]

* Roma Tre University
Department of Engineering - Section of Civil Engineering
Via Vito Volterra, 62, 00146 Rome, Italy
E-mail: stefano.desantis@uniroma3.it

[+] Roma Tre University
Department of Engineering - Section of Civil Engineering
Via Vito Volterra, 62, 00146 Rome, Italy
E-mail: gianmarco.defelice@uniroma3.it

Keywords: Masonry arches, fibre beams, composite materials, strengthening.

Abstract: *Composite materials are nowadays widely used to strengthen masonry structures and structural components such as arches and vaults. The scientific interest on these issues is increasing and new technologies are being developed, but reliable assessment procedures and robust analysis tools to verify the effectiveness of the strengthening still need to be fully defined.*
A modelling strategy based on the use of fibre beam elements is proposed in this work to study the behaviour of masonry arches strengthened with externally bonded composite materials. The method offers a good compromise between accuracy and simplicity such that the possible failure modes (hinge mechanism activation, crushing of masonry, sliding, rupture of the fibres and debonding) can be represented with limited computational efforts. The reliability of the proposed approach is first verified by comparison with experimental results. Numerical analyses on arches under different loading conditions and strengthening solutions are then performed to investigate the role played by the most relevant parameters on load carrying strength, displacement capacity and failure modes.

1 INTRODUCTION

Composite materials are nowadays widely used to strengthen masonry structures and structural components such as arches and vaults. The scientific interest on this topic is increasing and new technologies are being developed. Laboratory studies on reinforced arches have already shown that externally bonded reinforcement systems are able to provide a significant enhancement of the load carrying capacity and a reduction of the lateral thrust, without increasing the masses and respecting at the same time the original structural arch behaviour [1-4].
Both analytical and numerical approaches have been proposed for the structural analysis of reinforced arches structural elements, but reliable assessment procedures and robust analysis tools to verify the effectiveness of the strengthening still need to be fully defined. Analytical methods include similar versions of a modified mechanism method [5-6], in which the thrust line under the given external loads is calculated either starting from the hinge pattern of the unreinforced arch and eliminating the hinges whose development is prevented by the reinforcement [6] or by solving a constrained nonlinear optimization problem within a kinematic approach framework [5]. By doing so, the normal force and the bending moment are evaluated for each cross section of the arch and compared to its resisting properties, derived from the theory of reinforced concrete based on the principles of strain compatibility and force equilibrium.
Numerical methods have been proposed making use of both 1D and 2D finite elements [7-9], but the uncertainties in representing local phenomena (such as laminate debonding and arch failure by shear sliding) may strongly affect the reliability of the results, especially for simplified 1D approaches. On the other hand, 2D strategies allow for a more refined representation of the structure (including the mortar joints, the reinforcement layer and the matrix-substrate interface) but often need heavy computational efforts and the definition of a large number of input parameters.
A modelling strategy based on the use of fibre beam elements is proposed in this work to study the behaviour of masonry arches strengthened with externally bonded composite materials. The method, which has already been used to represent the static and dynamic behaviour of unreinforced masonry arches and arch bridges [10-12], is extended to include a simplified representation of the possible failure modes of the strengthened arch with low computational efforts. Its reliability is first verified by comparison with the experimental results presented in [3]. Numerical analyses under different loading conditions are then performed to investigate the role played by the strengthening configuration (intrados/extrados) and its stiffness on load carrying resistance, displacement capacity and failure mode.

2 FIBRE BEAM BASED MODELLING APPROACH

Starting from experimental results and numerical simulations of masonry elements under eccentric axial loads [13], the masonry arch is represented through nonlinear beam elements whose cross section is discretised into fibres (Figure 1). Uniaxial constitutive laws are assigned to the fibres, which makes it possible to represent the actual material behaviour with low computational efforts. In the present case, a modified Kent&Park model is used for masonry in compression, consisting of an ascending parabolic branch followed by a linear softening phase with no residual strength. The composite strip is included by

assigning to one fibre in the arch section a suitable constitutive law, which is elastic-brittle in tension and non resistant in compression.

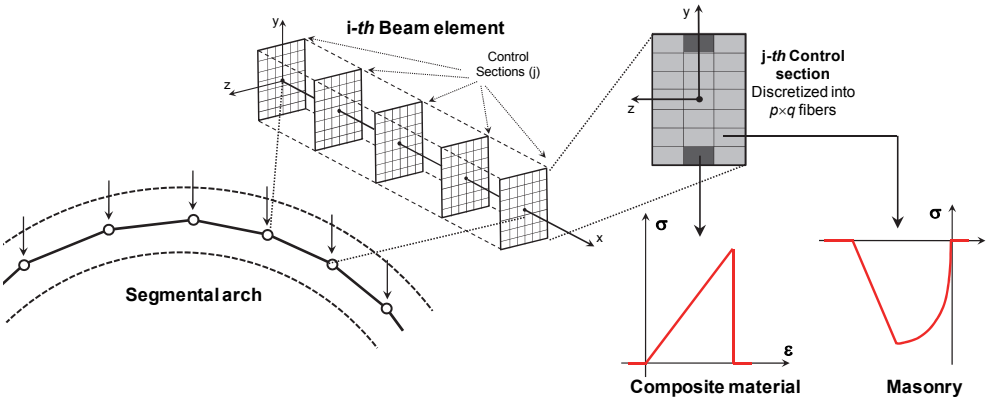

Figure 1: The fibre beam based modelling approach

The fibre beam model represents the failure modes of the reinforced arch as follows.
(i) Hinged mechanism development. It is automatically predicted by the fibre beam model. A strong concentration of curvature develops in the cross sections experiencing the highest load eccentricity, thus resulting in the development of hinges, which are spread over a number of control sections, and not concentrated in one single point, due to the continuum nature of the finite element method and to the material properties assigned to the fibres.
(ii) Crushing of masonry. It is accounted for through the stress-strain relationship assigned to the fibres to represent the local behaviour of masonry.
(iii) Tensile rupture of the fibre. It is accounted for through the constitutive law assigned to the fibres representing the composite material. As soon as rupture takes place, the contribution of the reinforcement suddenly disappears, due to the brittle nature of the composite material. Afterwards, the simulation continues with the other reinforcement strips which have not collapsed yet (if any) and the masonry core.
(iv) Laminate debonding from the masonry substrate. Since the fibre beam model is based on the plane section assumption, the fibres are not allowed to slide with respect to each other. Therefore, the debonding failure cannot be represented explicitly and is evaluated within an automated post-processing phase as follows. The stress in the fibre representing the composite material is recorded in each control section at each analysis step. The stress variation ($\Delta\sigma^j$) is computed between two sections (*i* and *j*) placed at a distance from each other equal to the effective anchorage length, evaluated starting from the properties of the composite and of the substrate according to [14]. The corresponding resultant force (V_d^i) is then derived by multiplying $\Delta\sigma^i$ by the cross section area of the reinforcement strip (A_f) and the average shear stress at the substrate-reinforcement interface (τ_d^i) is evaluated by dividing V_d^i by the interface area A_c:

$$\tau_d{}^i = \frac{V_d{}^i}{A_c} = \frac{\Delta\sigma^i A_f}{A_c} = \frac{(\sigma^j - \sigma^i)A_f}{A_c} \qquad (1)$$

This then compared to the ultimate stress value (τ_u), derived according to [14], which represents the maximum average interface shear stress on the effective anchorage length on a plane substrate. To account for the arch curvature, τ_u is multiplied by a scalar factor which includes the normal stress orthogonal to the arch extrados (σ_{ort}) and the tensile strength of masonry (f_{mt}), which is assumed to be 0.1 times the compressive strength:

$$\tau_{res} = \tau_u \left(1 - \frac{\sigma_{ort}}{f_{mt}}\right), \text{ where the normal stress is derived as: } \sigma_{ort} = \frac{F^i}{R \cdot \varphi \cdot b_f} \quad (2)$$

In Eqn. (2), R is the curvature radius of the arch, φ is the number of reinforcement strips, b_f is their width and F^i is the average tensile load between the considered control sections:

$$F^i = \frac{(\sigma^i + \sigma^j)A_f}{2} \quad (3)$$

The resisting shear stress on the curved surface is higher than that of the plane surface if $\sigma_{ort}<0$ (normal stresses oriented towards the arch, at the extrados) and lower if $\sigma_{ort}>0$ (normal stresses oriented outwards, at the intrados). Clearly, debonding occurs as soon as $\tau_d^i > \tau_{res}$ in the generic *i*-th control section of the arch.

(v) Shear failure of masonry. As the fibre beam model is not able to represent shear failure, it is evaluated within the post-processing phase as follows. According to [2], the shear strength of the *i*-th arch cross section at the *k*-th analysis step ($T_u^{i,k}$) is expressed as:

$$T_u^{i,k} = \mu \cdot C^{i,k} \quad (4)$$

In Eqn. (4), μ=0.6 is the friction coefficient and $C^{i,k}$ is the resultant of compressive stresses. Clearly, failure occurs as soon as the shear induced by loads ($T_d^{i,k}$) exceeds $T_u^{i,k}$.

3 COMPARISON WITH EXPERIMENTAL RESULTS

Aiming at validating the proposed modelling approach, the experimental tests presented in [3] are simulated. The tested structure is a catenary arch having 1.98m span, 10cm thickness, 20cm width and 49cm rise (Figure 2). The arch is made out of clay bricks with 43.3N/mm^2 compressive strength, 25×10^{3}N/mm^2 Young's modulus and 10.9N/mm^2 tensile strength and cement mortar with 8×10^{3}N/mm^2 Young's modulus. Bricks are 5cm thick, while the thickness of the mortar joints is about 1cm. The arch is built on concrete abutments connected to each other by means of steel C-beams to prevent relative movements. The load is applied monotonically at 3/4 span by means of an hydraulic jack resting on a flat steel plate. Different strengthening solutions making use of externally bonded composite material strips are considered such as intrados and extrados reinforcement, steel and carbon fibres, cementitious and polymeric matrices. Steel plates are also included in some specimens to anchor the reinforcement to the abutment and prevent debonding failure at the arch springing sections.

The arch is modelled with 80 nonlinear frame elements, whose section is discretised into 80×3 fibres. The end nodes are assumed as perfectly fixed, based on the experimental setup. A compressive strength of 35.1N/mm^2 and an initial stiffness of 17.8×10^{3}N/mm^2 are used for masonry starting from the geometric and mechanical properties of the materials (bricks

and mortar) by recurring to well-known homogenization principles and assuming ν_b=0.25 and ν_m=0.3 for the Poisson's ratios of brick and mortar, respectively. Finally, a deterioration rate η=2 is assumed, while the tensile strength is neglected. As for the reinforcement, the mechanical properties are derived starting from the characteristics of the materials (fibres and matrix) as well as of the composite systems (geometric ratios, textile equivalent thickness) according to the instruction provided by [14] and literature data (see, among others, [15]).

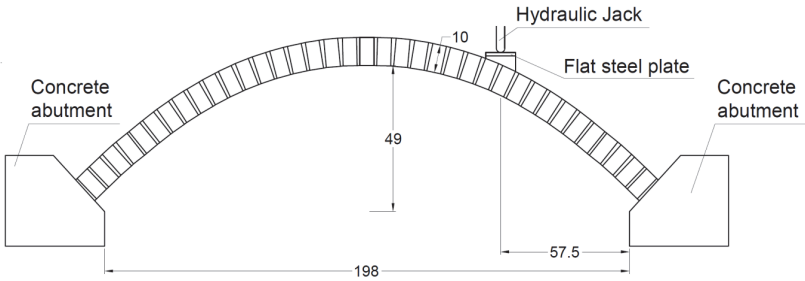

Figure 2: Strengthened masonry arch tested in laboratory [3]

All the arch fibre beams include the reinforcement, with the only exceptions of the first and last ones for the specimens which were not equipped with steel anchors, to account for the negligible contribution of the reinforcement in the vicinity of its end. The load is applied within a displacement controlled incremental static analysis in which geometric second order effects are taken into account by means of a corotational transformation rule.
The results of numerical simulations, compared to the experimental outcomes, are collected in Table 1. The unreinforced arch collapses under a load of 0.7kN and a four hinge mechanism develops. Both the maximum load and the location of the hinges are correctly predicted by the fibre beam model. The reinforcement applied to the arch extrados provides an increase of the ultimate load up to 9.1kN and more than 20kN for the arch without and with steel anchors, respectively. In both cases, shear failure occurs in the vicinity of the applied force (Figure 3a). On the contrary, if the reinforcement is applied to the intrados, the ultimate load is 10.1kN. Debonding failure occurs where curvature concentrates (Fig 3b), which is likely to be related to the orthogonal tensile stresses arising at the reinforcement-substrate interface resulting in a lower bond performance, as expected for intrados strengthening. As the identification of the collapse occurrence takes place within the post-processing phase, the load-displacement response curve predicted by the numerical model is not affected by shear sliding and laminate debonding failure modes taking place (Figure 3). Finally, if the composite material strips are applied to both intrados and extrados, the ultimate load is 20.9kN and sliding failure occurs, which slightly precedes debonding. The fibre beam model underestimates the experimental ultimate load in this case, which may be attributed to the difficulty in predicting the combined sliding-debonding failure mode observed in the laboratory.

Strengthening position	Strengthening Type	Experimental ultimate load	Numerical ultimate load	Experimental Failure mode	Numerical Failure mode
Unreinforced arch	-	0.71kN	0.69kN	Mechanism	Mechanism
Extrados	Cem. grout + steel cords	9.2kN	9.1kN	No clear failure mode	Shear Sliding
Extr. + Steel anchors	Cem. grout + steel cords	23.4kN	20.4kN	Shear Sliding	Shear Sliding
Intrados	Polym. resin + carbon fibres	12.3kN	10.1kN	Debonding	Debonding
Extr. + Intr.	Cem. grout + steel cords	33.0kN	20.9kN	Shear Sliding + Debonding	Sliding

Table 1: Comparison between experimental results [3] and numerical simulations with fibre beams for the strengthened arch under concentrated load at 3/4 span

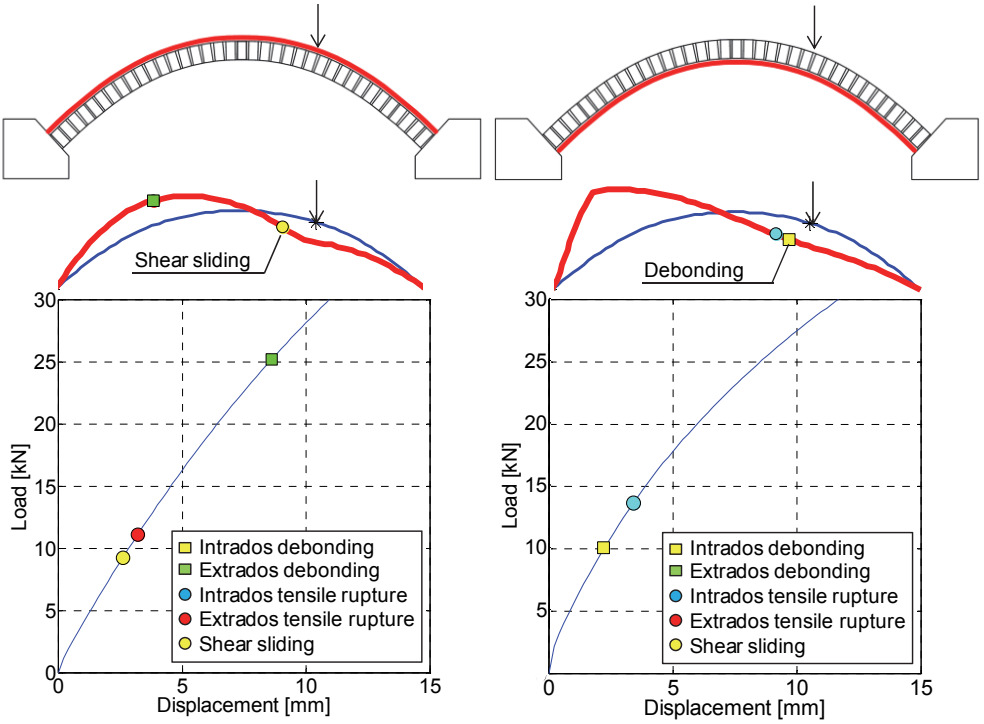

Figure 3: Collapse configurations and load-displacement curves of strengthened arches under concentrated load at 3/4 span: extrados (a) and intrados reinforcements (b)

4 NUMERICAL SIMULATIONS

In this section, the response of the strengthened masonry arch under distributed loads and vertical constrain movements are investigated through the fibre beam modelling approach.

The structure is the same catenary arch considered in the previous section while the reinforcement has a width of 15cm and is made out of inorganic matrix and steel cords with 635N/mm^2 tensile strength, 143×10^{3}N/mm^2 Young's modulus with 0.81mm^2 area each and 0.81mm equivalent tape thickness. Two densities are considered such as 4 cords/inch and 12 cords/inch to investigate the effect of reinforcement stiffness. The results of the numerical simulations are collected in Tables 2 and 3 for the distributed load and the constrain movement, respectively. Similarly to the concentrated load condition, a significant improvement in the load carrying capacity is provided by the reinforcement, ranging from 8.6 (intrados strengthening) to 17.7 (coupled intrados and extrados strengthening). Debonding failure occurs, as shear stress concentration under spread loads are lower than that under point forces. The effect of the strengthening is less evident for the arch under constrain displacement and a slight reduction of the displacement capacity is even found in the case of intrados reinforcement. Shear sliding occurs in the vicinity of the fixed abutment, which is typically a brittle phenomenon. Sensitivity analyses, however, suggest that this may be prevented by reducing the stiffness ratio between reinforcement layer and masonry substrate, which may be achieved by using lower density textiles or by interposing a deformable layer between substrate and matrix.

Strengthening position	Density: 4 cords/inch			Density: 12 cords/inch		
	Ultimate load	Increase	Failure mode	Ultimate load	Increase	Failure mode
Unreinforced arch	2.2kN	-	Mechanism	2.2kN	-	Mechanism
Extrados	30.0kN	13.6	Debonding	27.06kN	12.3	Debonding
Intrados	18.9kN	8.6	Debonding	17.16kN	7.8	Debonding
Extr. + Intr.	39.0kN	17.7	Debonding	34.98kN	15.9	Debonding

Table 2: Numerical simulations with the fibre beam model for the strengthened arch under distributed load on half span: load carrying capacity for different density reinforcements

Strengthening position	Density: 4 cords/inch			Density: 12 cords/inch		
	Max. displ.	Increase	Failure mode	Max. displ.	Increase	Failure mode
Unreinforced arch	1.28mm	-	Mechanism	1.28mm	-	Mechanism
Extrados	1.80mm	1.41	Shear Sliding	1.30mm	1.01	Mechanism
Intrados	1.2mm	0.96	Shear Sliding	1.35mm	1.05	Mechanism
Extr. + Intr.	1.85mm	1.44	Shear Sliding	1.39mm	1.08	Mechanism

Table 3: Numerical simulations with the fibre beam model for the strengthened arch under constrain settlement: displacement capacity for different density reinforcements

CONCLUSIONS

A fibre beam based approach is used to model masonry arches reinforced with externally bonded composite materials. The strategy provides a simplified bur reliable representation of the structural response and the possible failure modes within low computational efforts.
A satisfactory agreement is found between numerical simulations and experimental results in terms of ultimate load and failure modes, except when combined shear sliding-laminate debonding failure takes place, which is more difficult represent within a 1D approach.

A strong increase in the load carrying capacity is found for extrados and intrados reinforcements, under concentrated loads at 3/4 span and distributed loads on half span. Most times, failure occurs by laminate debonding, but shear sliding takes place under concentrated loads on arches reinforced at the extrados. Shear may be the critical failure mode also for strengthened arches subjected to constrain movements due to the stiffness increase provided by the reinforcement laminates. According to the preliminary results presented in this work, the displacement capacity is not significantly improved by the strengthening, which, on the contrary, may induce a brittle failure by shear sliding if high density textiles are used.

REFERENCES

[1] Valluzzi, M.R., Valdemarca, M., Modena, C. 2001. Behaviour of brick masonry vaults strenghtened with FRP laminates. *J Compos Constr* 5(3): 163-169.

[2] Foraboschi, P. 2004. Strengthening of masonry arches with fiber-reinforced polymer strips. *J Compos Constr, ASCE* 8(3): 191-202.

[3] Borri, A., Casadei, P., Castori, G., Hammond, J. 2009. Strengthening of brick masonry arches with externally bonded steel reinforced composites. *J Compos Constr, ASCE* 13(6): 468-475.

[4] Tao, Y., Stratford, T.J., Chen, J.F. 2011. Behaviour of a masonry arch bridge repaired using fibre-reinforced polymer composites. *Eng Struct* 33(5): 1594-1606.

[5] Chen, J.F. 2002. Load-bearing capacity of masonry arch bridges strengthened with fibre reifnroced polymer composites. *Adv Struct Eng* 5(1): 37-44.

[6] Briccoli Bati, S., Rovero, L. 2008. Towards a methodology for estimating strength and collapse mechanism in masonry arches strengthened with fibre reinforced polymer applied on external surfaces. *Mater Struct* 41(7): 1291-1306

[7] Basilio, I., Oliveira, D., Lourenço, P.B. 2004. Optimal FRP strengthening of masonry arches. *Proc of 13th Int. Brick Block Masonry Conf., Amsterdam, NL*.

[8] Drosopoulos, G.A., Stavroulakis, G.E., Massalas, C.V. 2007. FRP reinforcement of stone arch bridges: unilateral contact models and limit analysis. *Compos B* 38(2): 144-151.

[9] Elmalich, D., Rabinovitch, O. 2010. Nonlinear analysis of masonry arches strengthened with composite materials. *J Eng Mech, ASCE* 136(8): 996-1005.

[10] de Felice, G. 2009. Assessment of the load-carrying capacity of multi-span masonry arch bridges using fibre beam elements. *Eng Struct*31(8): 1634-1647.

[11] De Santis, S. 2011. Load carrying capability and seismic assessment of masonry bridges. *PhD Thesis*. Roma Tre University.

[12] De Santis, S., de Felice, G. 2013. An overview of railway masonry bridges with safety factor estimate. *Int J Architect Herit*. In press.

[13] de Felice, G., De Santis, S. 2010. Experimental and numerical response of arch bridge historic masonry under eccentric loading. *Int J Architect Herit* 4(2): 115-137.

[14] CNR DT 200 R1. 2012. Istruzioni per la progettazione, l'esecuzione ed il controllo di interventi di consolidamento statico mediante l'utilizzo di compositi fibrorinforzati.

[15] Carbone, I. 2010. Il problema della delaminazione nei compositi a matrice cementizia. *PhD Thesis*. Roma Tre University.